J Opt (September 2022) 51(3):699–706
https://doi.org/10.1007/s12596-021-00820-w

RESEARCH ARTICLE

Optical design of an antenna that is insensitive to decenters for laser communication

Jiake Wang[1,2] · Yang Wang[1,2] · Zhiyuan Gu[3] · Yuejiao Qiu[4] · Wenjun He[1,2]

Received: 17 August 2021 / Accepted: 29 December 2021 / Published online: 25 March 2022

Abstract In this paper, a laser communication antenna with two mirrors is designed. The decenters of the secondary mirror do not introduce field-linear coma, which reduces the antenna's sensitivity to misalignment, and we call it coma insensitive system. The conic coefficients of the primary and secondary mirrors of the coma insensitive system are different from those of the Cassegrain and Ritchey–Chretien systems. We derive the calculation formula of the coma insensitive system in detail based on the nodal aberration theory. Through a design example, the performance of the coma insensitive, Cassegrain and Ritchey–Chretien system in the nominal state and the secondary mirror decentered state is compared, and it is found that the aberration performance of the Cassegrain and Ritchey–Chretien system in the nominal state is much better than that of coma insensitive system. However, when the secondary mirror is decentered, the performance of Cassegrain and Ritchey–Chretien system is obviously inferior to coma insensitive system, and their rms spot diameter is about 2.8 times that of coma insensitive system.

✉ Yang Wang
wangyang@cust.edu.cn

1 School of Opto-Electronic Engineering, Changchun University of Science and Technology, Changchun 130022, China

2 Key Laboratory of Optoelectric Measurement and Optical Information Transmission Technology of Ministry of Education, Changchun University of Science and Technology, Changchun, China

3 Changchun Institute of Optics, Fine Mechanics and Physics, Chinese Academy of Sciences, Changchun 130033, China

4 Changchun Railway Traffic Group Co, Ltd., Changchun 130000, China

Keywords Optical design · Nodal aberration theory · Laser communication · Optical antenna · Two-mirror telescope · Coma · Misalignment

Introduction

With the development of space sensing technology, the amount of information transmitted by various spacecraft has increased exponentially. Space laser communication is the most promising space communication technology. Compared with traditional microwave communication, laser communication has the advantages of small divergence angle, fast transmission rate, large communication capacity and strong anti-electromagnetic interference performance, which is widely used in space communication [1–5].

In 2006, the forward link from ARTEMIS of the European Space Agency to OICETS of Japan used 2 Pulse Position Modulation format at 2.048 M bits/sec while the return link from OICETS to ARTEMIS used the Non-Return-to-Zero format at 49.3724 Mbits/sec [6]. In 2008, a duplex transmit data rate of 5.6 Gbps was achieved with a bit error better than 10^{-9} between two LEO satellites, NFIRE (USA) and TerraSAR-X (Germany) [7]. In 2013, the USA successfully performed the first time duplex laser communications between a space terminal (the Lunar Lasercom Space Terminal, LLST) and a primary ground terminal (the Lunar Lasercom Ground Terminal, LLGT). It constituted the longest-range laser communication link ever built and demonstrated the highest communication data rates at 622 Mbps ever achieved to or from the Moon [5, 8].

Optical antenna, also known as a receiving and transmitting telescope, is the core part of the laser communication terminal. The main function of the optical antenna is to transmit the optical signals which are carrying information to other terminals or analyze the optical signals from other terminals. The design of the terminal optical system usually needs to reach the diffraction limit, and the wave aberration is required to be less than 33 nm, which puts forward higher requirements on the optical design and alignment of the system [9]. In 2012, Cheng Yanyan designed a spaceborne laser communication terminal. The optical antenna adopted Cassegrain structure with parabolic primary mirror (PM) and secondary mirror(SM). The diameter of the PM is 200 mm, the field of view (FOV) is 2mrad, and the magnification is 10 ×, and the wave aberration is better than $\lambda/20$ (λ = 632.8 nm, similarly hereinafter) [10]. In 2018, Li Xiang designed a laser communication optical antenna, in which the parabolic PM is 150 mm, and the SM is designed with a 26 mm hyperboloid [11]. The FOV is 4mrad, the focal length is 1500 mm, the magnification is 15 ×, and the wave aberration is better than $\lambda/14$.

The wave aberration of optical antennas is not only limited by design residuals, but also affected by manufacture and alignment errors. The optical antenna with two mirrors has a simple structure and is often used in laser communication systems, so the alignment errors of the SM have a greater impact on the wave aberration of antenna. At the same time, gravity will also cause the secondary mirror to decenter, which will introduce misalignment aberrations such as coma. This will affect the actual wave aberration of the antenna. Therefore, reducing the decenter sensitivity of the SM from the process of optical design is an effective method to improve the antenna performance.

In this paper, to improve the as-built performance of optical antenna, we derive the calculation formulas for optical parameters of an antenna that is insensitive to decenters based on the nodal aberration theory. The simulation experiment is conducted to verify the relevant results.

Design of the optical antenna

Specifications of the optical antenna

In this paper, combined with the existing designs and the requirements of the laser communication terminal, the specifications are determined, as shown in Table 1.

Table 1 Specifications of the optical antenna

Parameter	Value
Magnification	$20^{\times}$
Entrance pupil diameter	60 mm
FOV	± 3 mrad
Wavelength	974 nm, 1550 nm
Wave aberration	less than 1/40 λ in ± 0.5 mrad FOV
	less than $1/20\lambda$ in ± 3 mrad FOV

Common form of telescope

The optical antenna needs to have a wave aberration better than $\lambda/20$ in 3 mrad FOV. It is difficult to meet the requirements with a single parabolic mirror, so the objective lens is designed with two mirrors. Commonly used two-mirror objectives include the classical Cassegrain telescope and its improved forms: Ritchey–Chretien (R–C) objective. The PM and SM of the two types have different conic coefficients. The PM of Cassegrain telescope is parabolic, the SM is hyperboloid, and the two mirrors correct spherical aberration independently; The PM and SM of the R–C telescope are both hyperboloids, and both third-order spherical aberration and coma are corrected in the system [12].

If only the third-order spherical aberration is required to be corrected at the system level, then there is one degree of freedom left for the conic coefficients of the primary and secondary mirrors. The following will study the use of the remaining degrees of freedom to realize the decenter insensitive design.

Optical parameters calculation of coma insensitive system

According to the requirements of antenna parameters, the aperture is 60 mm, and the angular magnification is 20 times. The focal length of the objective lens in this design is set to 600 mm, and the f-number is 10; the focal length of the eyepiece is 30 mm and the f-number is 10. The two-mirror telescope consists of a PM and a SM, as shown in Fig. 1.

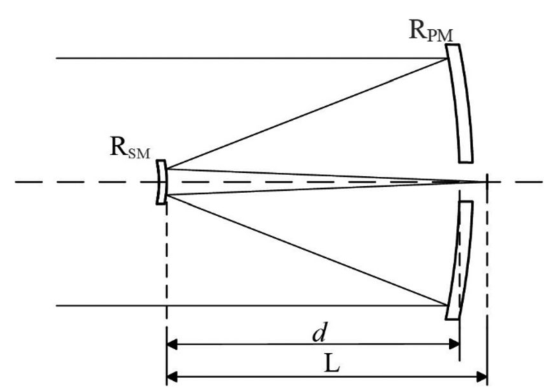

Fig. 1 Two-mirror objective

The radii of curvature of the PM (R_{PM}) and SM (R_{SM}) could be calculated by

$$R_{\mathrm{PM}} = \frac{2\mathrm{df}}{f - L} \tag{1}$$

$$R_{\mathrm{SM}} = \frac{2Ld}{-L + d + f} \tag{2}$$

where d is the interval between the PM and SM, f is the focal length of the telescope, and L is the back focal length of the telescope.

The third-order spherical aberration contributed by the spherical part of the PM($W_{040,PM}^{(sph)}$), the aspheric part of the PM($W_{040,\mathrm{PM}}^{(\mathrm{asph})}$), the spherical part of the SM($W_{040,\mathrm{SM}}^{(\mathrm{sph})}$) and the aspheric part of the SM($W_{040,\mathrm{SM}}^{(\mathrm{asph})}$) are as shown by

$$W_{040,\mathrm{PM}}^{(\mathrm{sph})} = \frac{1}{8}\left[-\left(\frac{y_1}{f}\right)^4 f\frac{m_2^3}{4}\right] \tag{3}$$

$$W_{040,\mathrm{PM}}^{(\mathrm{asph})} = \frac{1}{8}\left[-\left(\frac{y_1}{f}\right)^4 f\frac{m_2^3}{4}b_{s1}\right] \tag{4}$$

$$W_{040,\mathrm{SM}}^{(\mathrm{sph})} = \frac{1}{8}\left[\left(\frac{y_1}{f}\right)^4 L\frac{(m_2+1)^3}{4}\left(\frac{m_2-1}{m_2+1}\right)^2\right] \tag{5}$$

$$W_{040,\mathrm{SM}}^{(\mathrm{asph})} = \frac{1}{8}\left[\left(\frac{y_1}{f}\right)^4 L\frac{(m_2+1)^3}{4}b_{s2}\right] \tag{6}$$

where y_1 is the height of the marginal ray on the PM of the on-axis FOV, that is, the entrance pupil radius; b_{s1} and b_{s2} are the conic coefficients of the PM and SM, respectively, and m_2 is the magnification of the SM, which can be calculated by

$$m_2 = \frac{f - B}{d}. \tag{7}$$

After summing and simplifying Eqs. (3)–(6), the expression of the third-order spherical aberration of the two-mirror telescope system can be obtained, as shown by

$$W_{040}^{\mathrm{sys}} = \frac{-b_{s1}f(f-L)^3 + b_{s2}L(d+f-L)^3}{32d^3f^4} + \frac{L(d+f-L)(d-f+L)^2 - f(f-L)^3}{32d^3f^4}. \tag{8}$$

The nodal aberration theory is to study the aberration characteristics of an optical system with decentered and/or tilted optical elements. When the optical elements in a two-mirror system are misaligned, additional coma and astigmatism will be introduced, and coma is the main aberration. And the coma field is no longer symmetrically distributed around the optical axis. The coma node point, which is known as the FOV point where coma is zero, isn't located on-axis. The misaligned third-order coma field is superimposed on the original coma field, which can be expressed by

$$W_{\mathrm{COMA}_3} = \underbrace{\left(W_{131}\vec{H}\cdot\vec{\rho}\right)(\vec{\rho}\cdot\vec{\rho})}_{\text{original coma}} + \underbrace{\left(-\vec{A}_{131}\cdot\vec{\rho}\right)(\vec{\rho}\cdot\vec{\rho})}_{\text{misalignment−induced coma}} \tag{9}$$

where W_{131} is the sum of the third-order coma coefficients of the system, $\vec{H}$ is the FOV vector, and $\vec{\rho}$ is the pupil vector. In the misaligned two-mirror telescope, the PM can generally be regarded as the reference, and the SM is in a misaligned state. $\overrightarrow{A_{131}}$ could be expressed by

$$\vec{A}_{131} = \sum_j W_{131j}\vec{\sigma}_j = W_{131,SM}^{(sph)}\vec{\sigma}_{\mathrm{SM}}^{(sph)} + W_{131\mathrm{SM}}^{(asph)}\vec{\sigma}_{\mathrm{SM}}^{(asph)} \tag{10}$$

where $W_{131,SM}^{(sph)}$ and $W_{131,SM}^{(asph)}$ are the third-order coma coefficients contributed by the spherical part and the aspheric part of the SM, which are shown in Eqs. (11) and (12).

$$W_{131,SM}^{(sph)} = -\frac{u_{pr1}\,y_1^3\left(d + \frac{2df}{(L+d-f)} + \frac{L s_{pr1}}{f}\right)(L+d-f)^2(d-L+f)}{8\,d^3 f^3} \tag{11}$$

$$W_{131SM}^{(asph)} = -\frac{b_{s2}\,u_{pr1}\,y_1^3\left(L\,s_{pr1} + df\right)(d-L+f)^3}{8\,d^3 f^4} \tag{12}$$

where s_{pr1} is the distance between the entrance pupil and the PM, and u_{pr1} is the slope angle of the chief ray of the edge FOV, that is, the field angle. $\vec{\sigma}_{\mathrm{SM}}^{(sph)}$ and $\vec{\sigma}_{\mathrm{SM}}^{(asph)}$ are the aberration field decenter vectors of the spherical and aspherical parts of the SM, representing the distance between the center of symmetry of the aberration field and the chief ray of the on-axis FOV. They are related to the misalignments of the SM and can be expressed by

$$\vec{\sigma}_{\mathrm{SM}}^{(sph)} = -\frac{R_1\left(\mathrm{YDE} + \mathrm{ADE}\,R_2\right)}{u_{pr1}\left(dR_1 - 2d\,s_{pr1} + R_1R_2 + R_1\,s_{pr1} - 2R_2\,s_{pr1}\right)} \tag{13}$$

$$\vec{\sigma}_{SM}^{(asph)} = -\frac{\mathrm{YDE}\,R_1}{u_{pr1}\left(dR_1 - 2ds_{pr1} + R_1\,s_{pr1}\right)} \tag{14}$$

where YDE is the decenter of the SM in the y-axis direction, and ADE is the tilt of the SM along the x-axis[13]. Their definitions are the same as those in the optical design software Code V [14]. Equations (13) and (14) only consider the misalignments of the SM in the meridian plane, such simplified processing will not affect our analysis.

According to the above analysis, when $\vec{A}_{131}$ introduced by the misaligned SM is equal to 0, we can get

$$\frac{W_{131,\mathrm{SM}}^{(sph)}}{W_{131\mathrm{SM}}^{(asph)}} = -\frac{\vec{\sigma}_{\mathrm{SM}}^{(asph)}}{\vec{\sigma}_{\mathrm{SM}}^{(sph)}}. \tag{15}$$

Under the condition as shown by Eq. (15), there is no misaligned coma in the two-mirror system, that is, the misalignment of SM will not introduce coma. When the SM has both the YDE and ADE misalignments, it can be equivalently regarded as the SM rotating around a point in space. The distance between the point and the SM vertex is $L_{SM}^{(RP)}$, as shown by Eq. (16).

$$L_{\mathrm{SM}}^{(\mathrm{RP})} = -\frac{\mathrm{YDE_{SM}}}{\mathrm{ADE_{SM}}}. \tag{16}$$

Combining Eqs. (15) and (16), we can get

$$L_{\mathrm{SM}}^{(\mathrm{RP})} = -\frac{fR_2(d-f+L)^2\left(\frac{2df}{d-f+L}+d+\frac{Ls_{pr1}}{f}\right)}{(d(R_1-2s_{pr1})+R_1(R_2+s_{pr1})-2R_2s_{pr1})\left(\frac{b_{s2}(d+f-L)^2(df+Ls_{pr1})}{d(R_1-2s_{pr1})+R_1s_{pr1}}-\frac{(d-f+L)(Ls_{pr1}(d-f+L)+df(d+f+L))}{s_{pr1}(2d-R_1+2R_2)-R_1(d+R_2)}\right)}\frac{-b\pm\sqrt{b^2-4ac}}{2a}. \tag{17}$$

Therefore, the rotation of the SM around a point that is $L_{\mathrm{SM}}^{(\mathrm{RP})}$ from its vertex does not introduce misaligned coma, which is also called coma insensitive point. It can be seen from this property that when $L_{\mathrm{SM}}^{(\mathrm{RP})} = \infty$, it is equivalent to there will be no misaligned coma after the SM is decentered. In this way, we can get a two-mirror optical design that is not sensitive to decenter errors. Therefore, $W_{040}^{\mathrm{sys}} = 0$ can be used to make the system meet the condition of eliminating spherical aberration, and $L_{\mathrm{SM}}^{(\mathrm{RP})} = \infty$ can be set so that the system does not introduce coma when the SM is decentered. After solving these two equations, the solutions of the conic coefficients of the PM and SM can be obtained, as shown in Eq. (18).

$$b_{s1} = \frac{2L}{f} - \frac{2Ld^2}{f(L-f)^2} - 1 \tag{18}$$

$$b_{s2} = \frac{-d-L+f}{d-L+f}. \tag{19}$$

Using Eqs. (1), (2), (18) and (19), we can obtain the solution of the optical design parameters of the two-mirror antenna without introducing coma when the secondary mirror is decentered.

Design result of the antenna

When designing a two-mirror antenna, we can set $d = -75$ mm, $L = 82$ mm, $f = 600$ mm, and we can obtain the optical design parameters of the antenna, as shown in Table 2. The optical structure is shown in Fig. 2.

The coma distribution for full FOV of coma insensitive system is shown in Fig. 3a (1 wave = 587.56 nm, similar hereafter), and the rms spot diagram distribution is shown in Fig. 4a. It can be seen from the figure that the coma insensitive system achieves complete correction of third-order spherical aberration, the residual aberration of the on-axis FOV is high-order spherical aberration, and the main residual aberration of the off-axis FOV is coma.

For comparison, we also designed a Cassegrain system and an R–C system according to the conditions of

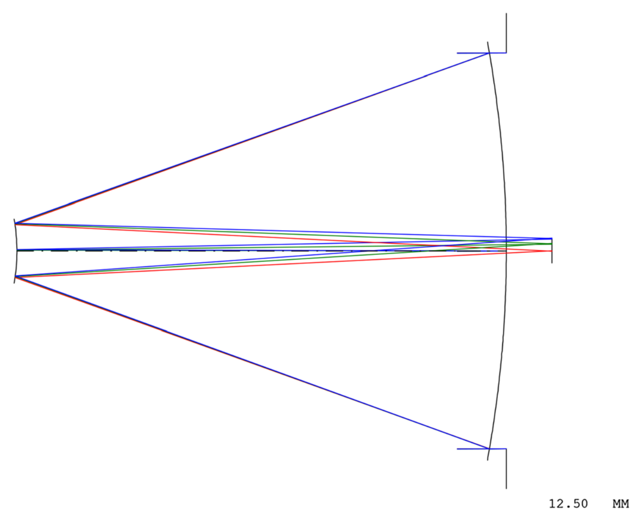

Fig. 2 Optical layout of the two-mirror antenna

Table 2 Parameters of the two-mirror antenna

Surface no.	Radius of curvature (mm)	Thickness (mm)	Conic coefficient
PM(stop)	−173.7452	− 75	− 0.7324
SM	−27.7652	82	1.3386

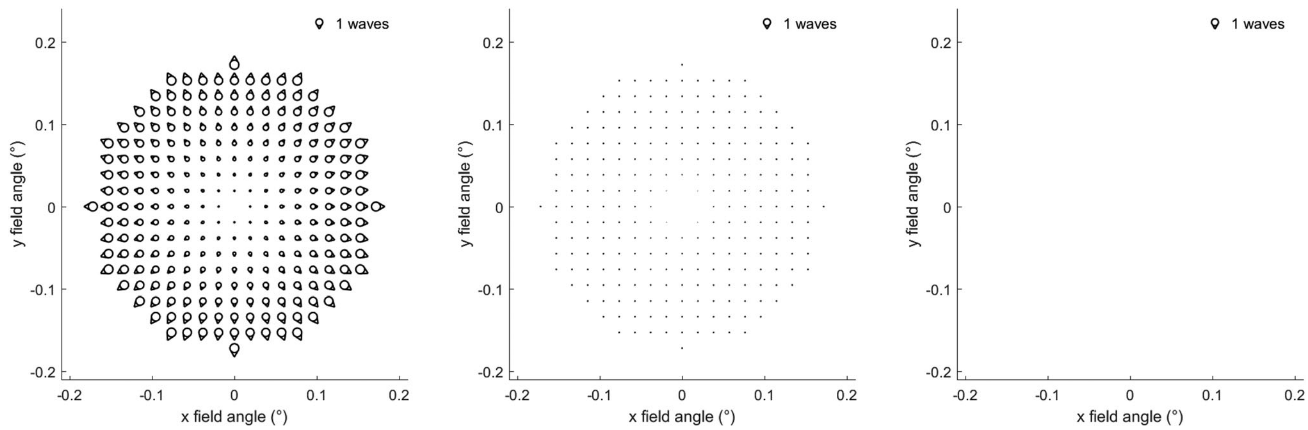

(a) **(b)** **(c)**

Fig. 3 The coma fields of **a** coma insensitive, **b** Cassegrain and **c** R–C system in the nominal state

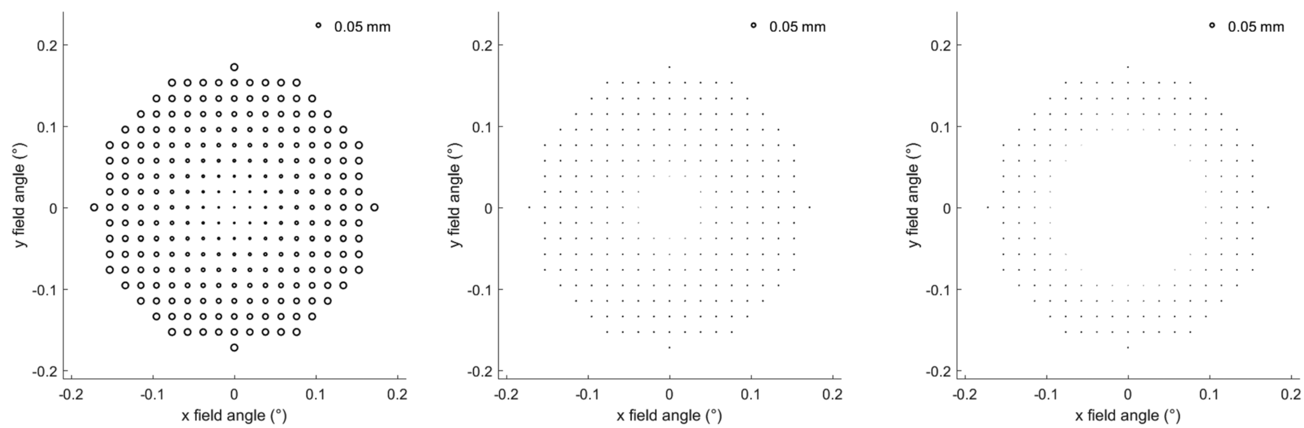

(a) **(b)** **(c)**

Fig. 4 The rms spot diameter fields of **a** coma insensitive, **b** Cassegrain and **c** R–C system in the nominal state

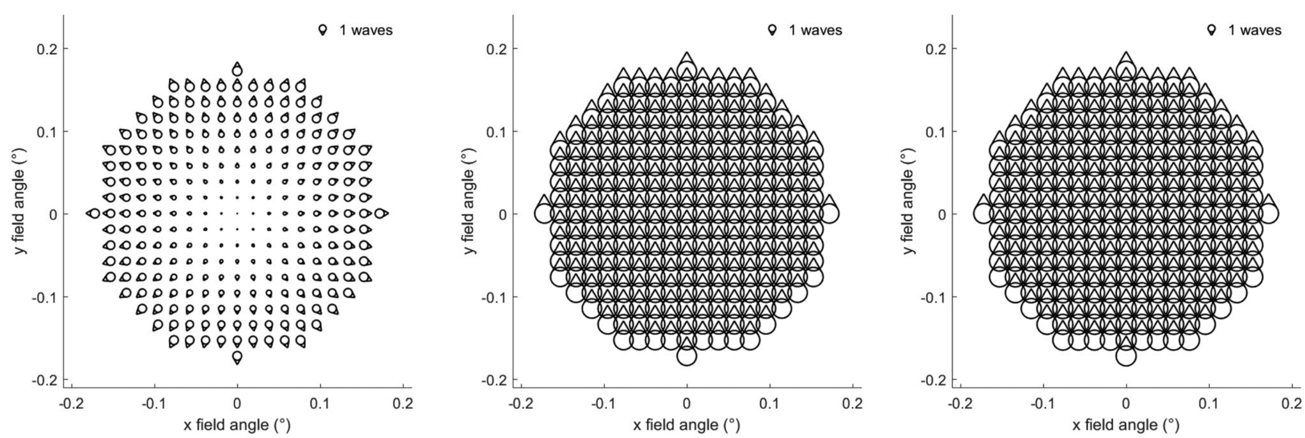

(a) **(b)** **(c)**

Fig. 5 The coma fields of **a** coma insensitive, **b** Cassegrain and **c** R–C system in the misaligned state (the secondary mirror is decentered by 0.5 mm)

$d = -75$ mm, $L = 82$ mm and $f = 600$ mm. All three systems realize the correction of third-order spherical aberration. The difference between these two systems and the coma insensitive system is only the conic coefficients of the PM and SM. Their coma distributions for full FOV are shown in Fig. 3b and c, respectively, and the rms spot diameter distributions are shown in Fig. 4b and c, respectively. It can be seen from the figures that the average rms spot diameter of the Cassegrain system and R–C system is 0.001 mm, while that of the coma insensitive system is 0.055 mm. The image quality of Cassegrain system and R–C system is significantly better than that of coma insensitive system. The reason is that the third-order coma in the Cassegrain system is small, and the R–C system also corrects the third-order coma in addition to correcting the third-order spherical aberration.

The SMs of the three systems are decentered by 0.5 mm along the *y* forward direction to verify the influence of the decenter errors. The coma distribution of the three systems is obtained as shown in Fig. 5, and the rms spot diameter distribution is shown in Fig. 6.

It can be seen from the figures that after the SM is decentered by 0.5 mm, the coma distribution and rms spot diameter distribution of the coma insensitive system are basically unchanged and still present a rotationally symmetrical distribution. However, after the SMs of Cassegrain and R–C are misaligned, the coma field shows an obvious field-linear coma, and the spot field also has an approximately uniform distribution. The detailed data is shown in Table 3. Even for a decenter of 0.5 mm (this value is a relatively large value for both gravity deformation and adjustment errors), the decenter of the secondary mirror in the coma insensitive system has minimal impact on the image quality, and the coma, spherical aberration, astigmatism and rms spot diameter are basically unchanged, as shown in Table 3 and Fig. 7.

From the above analysis, we can see that the design image quality of Cassegrain and R–C system is better than that of coma insensitive, but the image quality shows a great degree of deterioration after the secondary mirror is decentered. Their average rms spot diameter increases to about 0.16 mm, which is 2.8 times that of the misaligned coma insensitive system. It can be seen that although the design residual aberration of the coma insensitive system is large, the SM is very insensitive to decenter errors. Therefore, when the SM has gravity displacement or large adjustment errors, the system image quality is more stable,

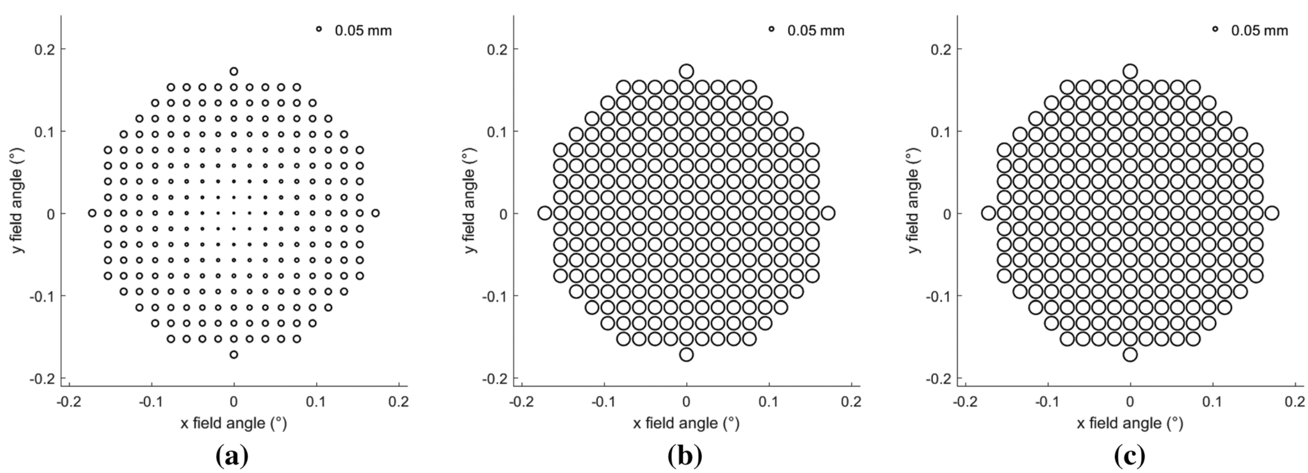

Fig. 6 The rms spot diameter fields of **a** coma insensitive, **b** Cassegrain and **c** R–C system in the misaligned state (the secondary mirror is decentered by 0.5 mm)

Table 3 The average coma, spherical aberration, astigmatism and rms spot diameter for full field of the three systems in nominal state and when the secondary mirror decentered by 0.5 mm

	Coma insensitive		Cassegrain		R–C	
	Nominal state	SM is decentered	Nominal state	SM is decentered	Nominal state	SM is decentered
Coma/waves	0.860	0.866	0.022	2.802	0.000	2.873
Spherical aberration/waves	0.092	0.093	0	0.018	0	0.019
Astigmatism/waves	0.033	0.428	0.018	0.087	0.019	0.098
rms spot diameter /mm	0.055	0.057	0.001	0.161	0.001	0.164

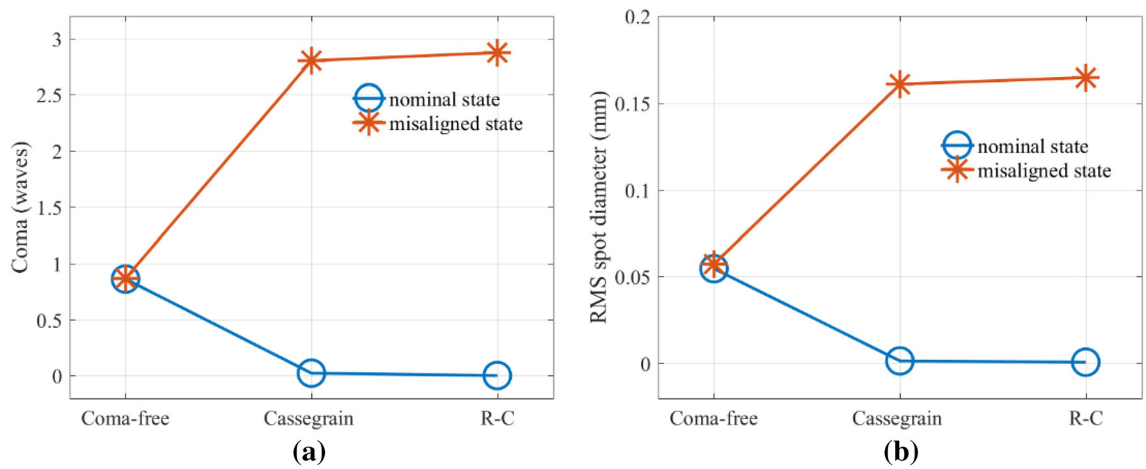

Fig. 7 The average coma and rms spot diameter for full field of the three systems in nominal state and when the secondary mirror decentered by 0.5 mm: **a** coma **b** RMS spot diameter

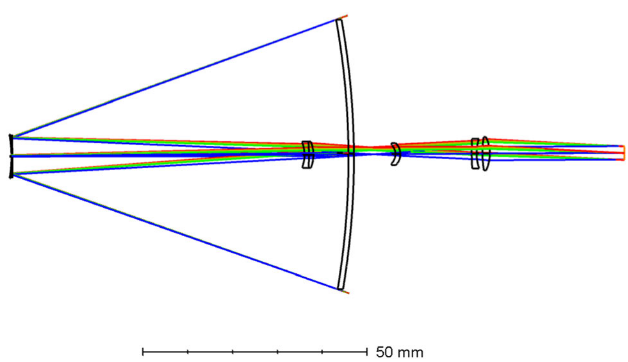

Fig. 8 The optical system obtained by combining the telescope and eyepiece

and the actual performance is better than the Cassegrain and R–C system.

Design of the eyepieces

The eyepiece can collimate the image of the telescope at an angular magnification of 20 times, and it can also correct the residual aberration of the telescope, mainly including third-order coma and field curvature. After optimization, an eyepiece is designed with 5 lens. The combined structure of the telescope and eyepiece is shown in Fig. 8, and the wave aberration the system is shown in Fig. 9.

As can be seen in Fig. 9a, the wave aberration is less than 0.01λ in 0.5 mrad FOV for both 1550 nm and 974 nm. In the 3mrad FOV, the wave aberration of 1550 nm is less than 0.02λ, and the wave aberration of 974 nm is less than 0.03λ, which all meet the design requirements. It can be seen from Fig. 9b, if the SM is decentered by 0.5 mm, the system wave aberration could be restored to the design state by adjusting the eyepiece.

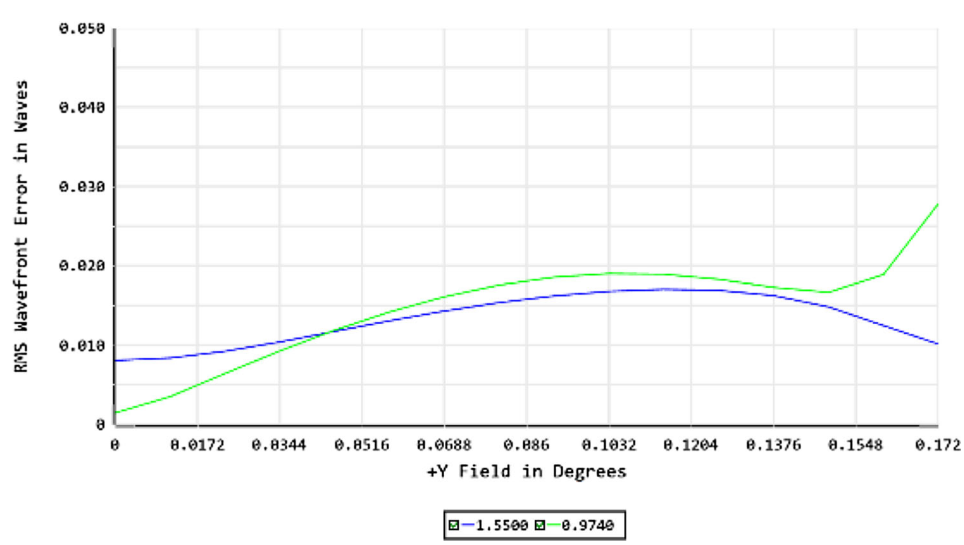

Fig. 9 Wave aberration vs. field of view: **a** nominal system and **b** the SM decentered by 0.5 mm

Conclusions

This paper uses the nodal aberration theory to design a laser communication antenna, which is composed of two-mirror telescope and a transmissive eyepiece. The conic coefficients of the PM and SM in the telescope are different from that of the Cassegrain system and the R–C system. The optical antenna corrects the system's third-order spherical aberration, and its wave aberration is not insensitive to the decenter errors of the SM. This paper derives the calculation method of the optical parameters of the optical antenna. The coma field and the rms spot diameter are compared between the coma insensitive, Cassegrain and R–C system in the nominal state and the misalignment state. The results show that in the nominal state, due to the large residual third-order coma of the coma insensitive system, the wave aberration is about 50 times that of the Cassegrain and R–C systems. When the SM is decentered by 0.5 mm, the coma field and rms spot diameter of the coma insensitive system basically do not change, but the image quality of the Cassegrain and R–C system has a large degradation. The average rms spot diameter of the Cassegrain and R–C system is about 2.8 times that of the coma insensitive system. The results show that the aberration of the coma insensitive system is insensitive to the decenter of the SM. In this paper, the eyepiece is also designed. The residual third-order coma and field curvature of the telescope can be corrected by the eyepiece, which could achieve a $20^{\times}$ angular magnification. The performance of the optical antenna with coma insensitive system is more stable than the Cassegrain and R–C system when there is large gravity deformation or alignment error, so it is more suitable for harsh environments and can greatly reduce the difficulty of system alignment.

Acknowledgements This research was funded by National Natural Science Foundation of China (NSFC), Grant Numbers are 61805025 and 62105331.

References

1. G. Duorui, Li. Tianlun, S. Yue, Latest developments and trends of space laser communication. Chinese Opt. **11**(6), 901–913 (2018)
2. J. Huilin, An. Yan, Z. Yanlin, Analysis of the status quo, development trend and key technologies of space laser communication. J. Spacettc TT&C Technol **34**, 207–217 (2015)
3. X. Sun, R. Skillman, E. Hoffman, Free space laser communication experiments from Earth to the Lunar Reconnaissance Orbiter in lunar orbit. Opt. Express **21**(2), 1865 (2013)
4. Z. Fei, G. Shijie, S. Xiaogang, Development status and trend of airborne laser communication terminals. Chinese Opt. **9**(1), 65–73 (2016)
5. D.M. Cornwell, Proc Spie. NASA's optical communications program for 2015 and beyond, 9354 (2015)
6. AT Jono, et al., Free-Space Laser Communication Technologies XIX and Atmospheric Propagation of Electromagnetic Waves International Society for Optics and Photonics. Overview of the inter-orbit and orbit-to-ground laser communication demonstration by OICETS (2007)
7. B. Smutny, et al., Proc Spie. 5.6 Gbps optical intersatellite communication link. 7199 (2009)
8. D.M. Boroson, B.S. Robinson, D.V. Murphy, et al., International Society for Optics and Photonics. Overview and results of the Lunar Laser Communication Demonstration (2014)
9. H. Hemmati, *Near-earth laser communications* (CRC Press, 2020)
10. Y. Cheng, Xi'an Institute of Optics and Precision Mechanics Chinese Academy of Science (2012)
11. L. Xiang, L. Ming, L. Xiaoming et al., Laser and optoelectronics progress. Des. Multipurp. Opt. Antenna Laser Commun. **55**, 020602 (2018)
12. Burley D et al (1999) Adv. Modern Eng. Math.
13. K.P. Thompson et al., Real-ray-based method for locating individual surface aberration field centers in imaging optical systems without rotational symmetry. J. Opt. Soc. Am. A **26**(6), 1503–1517 (2009)
14. CODE V Lens System Setup Reference Manual (Version 11.0)